ISSN 0036-0236, Russian Journal of Inorganic Chemistry, 2016, Vol. 61, No. 11, pp. 1451–1458. © Pleiades Publishing, Ltd., 2016.
Original Russian Text © D.A. Zherebtsov, S.A. Kulikovskikh, V.V. Viktorov, D.A. Uchaev, O.Yu. Desyatkina, I.I. Yangil'dina, E.A. Belaya, A.M. Kolmogortsev, K.R. Smolyakova, 2016, published in Zhurnal Neorganicheskoi Khimii, 2016, Vol. 61, No. 11, pp. 1506–1514.

PHYSICAL METHODS OF INVESTIGATION

Synthesis of Nanodispersed Anatase by Tetrabutoxy Titanium Hydrolysis

D. A. Zherebtsov[a, *], S. A. Kulikovskikh[b], V. V. Viktorov[b], D. A. Uchaev[a], O. Yu. Desyatkina[a], I. I. Yangil'dina[a], E. A. Belaya[c], A. M. Kolmogortsev[d], and K. R. Smolyakova[a]

[a] *South Ural State University, Chelyabinsk, 454080 Russia*
[b] *Chelyabinsk State Pedagogical University, Chelyabinsk, 454080 Russia*
[c] *Chelyabinsk State University, Chelyabinsk, 454001 Russia*
[d] *Snezhinsk Physics and Technology Institute, A Branch of National Research Nuclear University "MEPhI" (Moscow Engineering and Physics Institute), Snezhinsk, Chelyabinsk oblast, 456776 Russia*
**e-mail: zherebtsov_da@yahoo.com*

Received October 19, 2015

Abstract—Nanodispersed titanium oxyhydrate was obtained by tetrabutoxy titanium hydrolysis in the presence of a chelating agent, acetylacetone. The introduction of a chelating agent to tetrabutoxy titanium hydrolysis in a water–ethanol mixture allows one to control the hydrolysis rate. According to X-ray powder diffraction data, amorphous titanium oxyhydrate after annealing at 400°C transforms to anatase, the crystallites of which are 6.2–8.4 nm in size. Transmission electron microscopy showed that the anatase particles are close to spheres 5–9 nm in diameter. The amorphous materials were studied by differential thermal analysis, thermogravimetric analysis, and mass spectrometric analysis of released gases. The benzene adsorption by the produced materials was determined. The nitrogen adsorption isotherms of two samples were constructed, and the specific surface area of the anatase particles and the pore size were found (148.5 and 98 m^2/g, and 4.4 and 4.0 nm, respectively).

DOI: 10.1134/S003602361611022X

Titanium dioxide is one of the most important oxide materials used in many areas, such as catalysis; photocatalysis; and production of pigments, solar cells, self-cleaning coatings, and photovoltaic cells [1–4]. Currently, significant effort is made to create finely dispersed and porous materials based on it [5, 6] and develop their synthesis technologies [2, 6–8]. One of the most promising methods for producing titanium dioxide is hydrolysis of titanium alkoxides, in particular, tetrabutoxy titanium (TBT), which has still been insufficiently studied.

The purpose of this work was the investigation of the interaction of TBT with a chelating agent—acetylacetone (acac)—and a hydrolyzing aqueous ethanol solution to produce nanodispersed titanium oxyhydrate and then titanium oxide and the determination of the effect of the acetylacetone and water concentrations on the morphology and properties of titanium oxide.

EXPERIMENTAL

In the experiments, we used TDT, acac, and ethanol (96 vol %) (all analytically pure), and also distilled water and aqueous ammonia (25%).

Nanodispersed TiO_2 was synthesized at various contents of the stabilizing and hydrolyzing components (Table 1).

The synthesis was performed in two stages: initially, samples IY01–IY09 were prepared, and in a week, samples IY10–IY20 were produced. A TDT–acac solution (solution A) and ethanol–water solution (solution B) were prepared separately and then mixed with each other. This resulted in the formation of either a white polydisperse precipitate, or a sol, or a yellow solution. The white polydisperse precipitate of titanium oxyhydrate was obtained in samples with the lowest (0.05 mL) acac content. The yellow solution formed in samples with the highest (0.4 mL) acac content. In solutions containing 0.1 and 0.2 mL acac, the changes during the hydrolysis were intermediate.

At this stage, the particle size of the sol in samples IY02, 03, 04, 06, 07, and 08 was determined by dynamic light scattering with a Microtrac Nanotrac 253 Ultra laser particle-size analyzer.

In all the solutions with high acac concentrations, no visible changes occurred for 7 days, and to accelerate reaching equilibrium, samples IY01–IY09 were kept in a sealed container for 2 days in a drying cabinet at 70°C. After that, the samples containing a layer of

Table 1. Composition of samples, mL

Sample	Solutions A		Solutions B	
	TBT, mL	acac, mL	EtOH, mL	H_2O, mL
IY01	1	0.05	5	0
IY02	1	0.1	5	0
IY03	1	0.2	5	0
IY04	1	0.4	5	0
IY05	1	0.05	5	0.5
IY06	1	0.1	5	0.5
IY07	1	0.2	5	0.5
IY08	1	0.4	5	0.5
IY09	1	0.05	5	1
IY10	1	0.1	5	1
IY11	1	0.2	5	1
IY12	1	0.4	5	1
IY13	1	0.05	5	2
IY14	1	0.1	5	2
IY15	1	0.2	5	2
IY16	1	0.4	5	2
IY17	1	0.05	5	4
IY18	1	0.1	5	4
IY19	1	0.2	5	4
IY20	1	0.4	5	4

nonhydrolyzed TBT (5–70% of the initial TBT) at their bottoms transformed to a homogeneous solution or a homogeneous gel (Table 2). Samples IY10–IY20 were also placed in a drying cabinet at 70°C soon after mixing solutions A and B.

Because a yellowish (a sign of incomplete hydrolysis) solution occurred in most samples even after keeping them at 70°C, hydrolyzing agents were additionally introduced to the samples to complete hydrolysis (Table 3). Samples IY03, 04, and 08 (with the highest acac content) after hydrolysis with aqueous ammonia (Table 3) were homogeneous nontransparent gels, and in the samples with the lowest acac content, the precipitate was not homogeneous. For example, only 60% of sample IY01 was gel-like, and this gel formed in the solution over the polydisperse precipitate. This was due to the low content of the initial TBT in the solution of the initial precipitate. Solutions with higher acac contents passed the stages of thickening and gelation more slowly. For samples IY01, 02, 06, and 07, solutions were saturated in an atmosphere of water vapor and ammonia (in a desiccator).

The yellow solutions stable to hydrolysis at 70°C were further significantly diluted with water.

In samples IY11 and 15, about a half of TBT transformed to a semitransparent gel, which was dried and studied. The yellow solution over the gel was poured into a large volume of water (Table 3); the obtained solution was not changed to a precipitate until the end of the experiment and was not studied (to the end of the name of such samples, the letter *s* was added).

The solutions with the highest acac content (IY11, 12, 15, 16, 19, and 20) were poured while intensely stirring to a large (250–500 mL) volume of a water. In pouring a portion of a water–alcohol solution of TBT into water, at the moment of contact of two liquids, an opalescent precipitate formed for a short time, which completely dissolved while stirring in 2–10 s. This is indicative of a complex hydrolysis mechanism, which

Table 2. Visual changes in samples at the second stage of hydrolysis (in 2 days at 70°C)

H_2O	acac			
	0.05	0.1	0.2	0.4
0	IY01 Pale-yellow solution over polydisperse white precipitate	IY02 Yellow solution, gel	IY03 Yellow solution, gel	IY04 Dark-yellow solution
0.5	IY05 Pale-yellow solution over polydisperse white precipitate	IY06 Yellow solution, gel	IY07 Yellow solution, gel	IY08 Yellow solution
1.0	IY09 Transparent solution over polydisperse white precipitate	IY10 Pale-yellow solution over TBT (60% at bottom), sol in solution	IY11 Pale-yellow solution over TBT (40% at bottom), sol in solution	IY12 Yellow solution
2.0	IY13 Transparent solution over polydisperse white precipitate	IY14 Pale-yellow solution over TBT (50% at bottom)	IY15 Yellow solution over TBT (30% at bottom)	IY16 Yellow solution
4.0	IY17 Transparent solution over polydisperse white precipitate	IY18 Yellowish solution over TBT (40% at bottom)	IY19 Yellow solution over TBT (20% at bottom)	IY20 Yellow solution

Table 3. Visual changes in samples at the third stage of hydrolysis

Sample	Additional operation of hydrolysis	Result
IY01	Placement in desiccator with 10% ammonia	Transparent solution, 60% of transparent gel over polydisperse white precipitate
IY02	Placement in desiccator with 10% ammonia	Yellowish solution, transparent gel
IY03	Addition of 4 mL of 10% NH_3	Yellowish solution, nontransparent gel
IY04	Addition of 2 mL of 10% NH_3 + 2 mL EtOH	Yellow solution, transparent gel
IY05	Addition of 2 mL of 10% NH_3 + 2 mL EtOH	Transparent solution with voluminous precipitate
IY06	Placement in desiccator with 10% ammonia	Yellowish solution, gel
IY07	Placement in desiccator with 10% ammonia	Yellow solution, gel
IY08	Addition of 4 mL of 10% NH_3	Yellow solution, nontransparent gel
IY09	Addition of 2 mL of 10% NH_3 + 2 mL EtOH	Transparent solution with voluminous polydisperse white precipitate
IY11p	Addition of 250 mL of H_2O and 12 mL of NH_3	Solution, formation of short-lived opalescent precipitate. In 6 months, sol (in decanted part of sample)
IY12	Addition of 250 mL of H_2O and 12 mL of NH_3	Solution, formation of short-lived opalescent precipitate. In 3 months, precipitate
IY15p	Addition of 500 mL of H_2O and 12 mL of NH_3	Solution, formation of short-lived opalescent precipitate. In 6 months, transparent solution (in decanted part of sample)
IY16	Addition of 500 mL of H_2O and 12 mL of NH_3	Solution, formation of short-lived opalescent precipitate. In 6 months, sol
IY19	Addition of 350 mL of H_2O and placement in drying cabinet at 70°C	Solution, formation of short-lived opalescent precipitate. In 2 h, stable sol. In 1 day, gel
IY20	Addition of 350 mL of H_2O and placement in drying cabinet at 70°C	Solution, formation of short-lived opalescent precipitate. In 2 h, gel

passes through the stage of the formation of metastable short-lived products. Because further, for 20 min, these solutions experienced no visible changes, solutions IY15, 16, 19, and 20 were placed in a drying cabinet at 80°C. In 2 h, the solutions had been hydrolyzed to form a gel throughout the solution volume, although the solid phase content in the liquid was very low. Next, these samples were kept at 80°C for 1 h for hydrolysis to be completed. Aging of the gel led to its consolidation and settling to the bottom.

The obtained gel samples were dried at room temperature to an air-dry state and then at 50, 100, and 400°C for 1 day at each stage.

After annealing at 400°C, the samples were investigated by X-ray powder diffraction analysis (Rigaku Ultima IV diffractometer), scanning electron microscopy (Jeol JSM 7001F microscope), and transmission electron microscopy (Eva 120 Carl Zeiss microscope). Additionally, samples IY12, 19, and 20, which were not subjected to drying at >100°C, were studied by synchronous thermal analysis (Netzsch STA 449C Jupiter thermal analyzer) combined with mass spectrometry of released gases (Netzsch QMS 403C Aeolos mass spectrometer). The adsorption capacity of all the samples was found from the benzene adsorption according to a published procedure [9].

Samples IY07 and 08, which formed homogeneous transparent and nontransparent gels, respectively, were studied with a Micromeritics ASAP 2020 surface area and porosity analyzer allowing one to obtain the nitrogen adsorption–desorption isotherms at liquid nitrogen temperature, determine the specific surface area, and analyze the micro- and mesopore size distribution.

RESULTS AND DISCUSSION

In the sols and the solutions over the gel precipitates, by dynamic light scattering, the sizes of suspended particles were measured in 15 and 120 h after mixing solutions A and B. In this period, while keeping samples at room temperature, the sol particle size of samples IY02, 03, 04, 06, 07, and 08 ranged from 3 nm (samples IY04 and 08) to 8 nm (samples IY02 and 06), very slightly increasing with time. This indicated that, first, the presence of acac favors a decrease in the particle size, and second, the formation of these particles lasts less than 15 h. The X-ray powder diffraction anal-

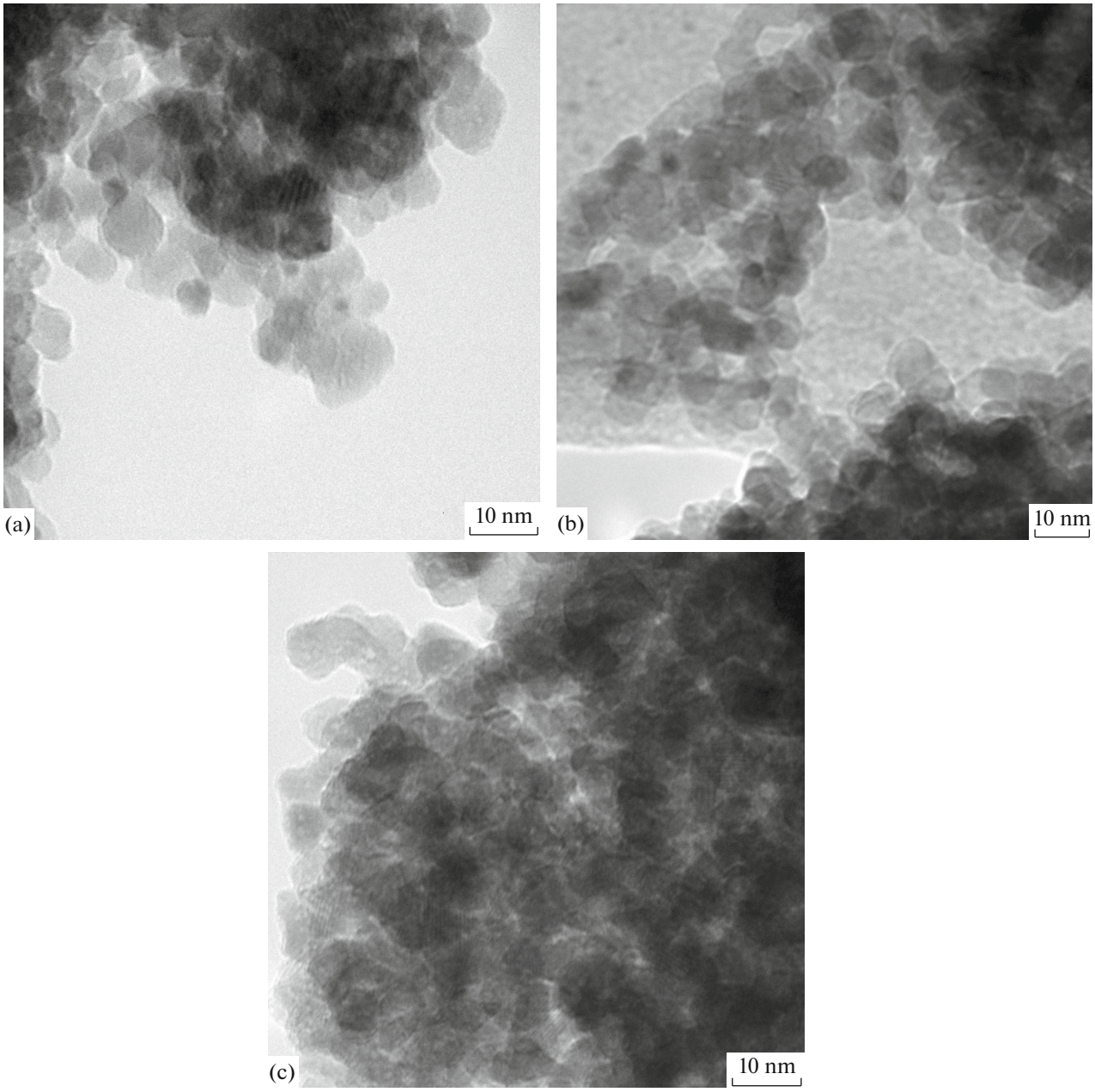

Fig. 1. Morphology of samples (a) IY02, (b) 03, and (c) 04 after treatment at 400°C according to transmission electron microscopy data.

ysis showed that they have no crystal structure. The size of amorphous particles in the solution is close to the size of the anatase particles forming after annealing (Figs. 1, 2). The morphology of samples after treatment at 400°C was examined by scanning and transmission electron spectroscopy. The anatase particles are distorted spheres 5–9 nm in diameter (Fig. 1). The scanning electron spectroscopy demonstrated that all the xerogel samples have the same morphology in the form of densely packed spherical particles of the size close to that of the particles of sample IY20 (Fig. 2a).

The thermal and thermogravimetric analyses of sample IY12 determined the completeness of TBT hydrolysis and the temperatures of the removal of residual organic groups (Fig. 3) on heating in air at a rate of 10°C/min. The data obtained suggest that the decomposition occurs in four stages: at 22–210, 210–320, 320–500, and 500–1100°C. The total weight loss at a temperature below 1100°C was 21.4 wt %, and the weight losses at each of the stages were 11.0, 3.2, 4.8, and 2.4 wt %. The mass spectrometry of the gaseous products of the decomposition showed that, at 100–210°C, water, butanol, acac, and ethanol are primarily

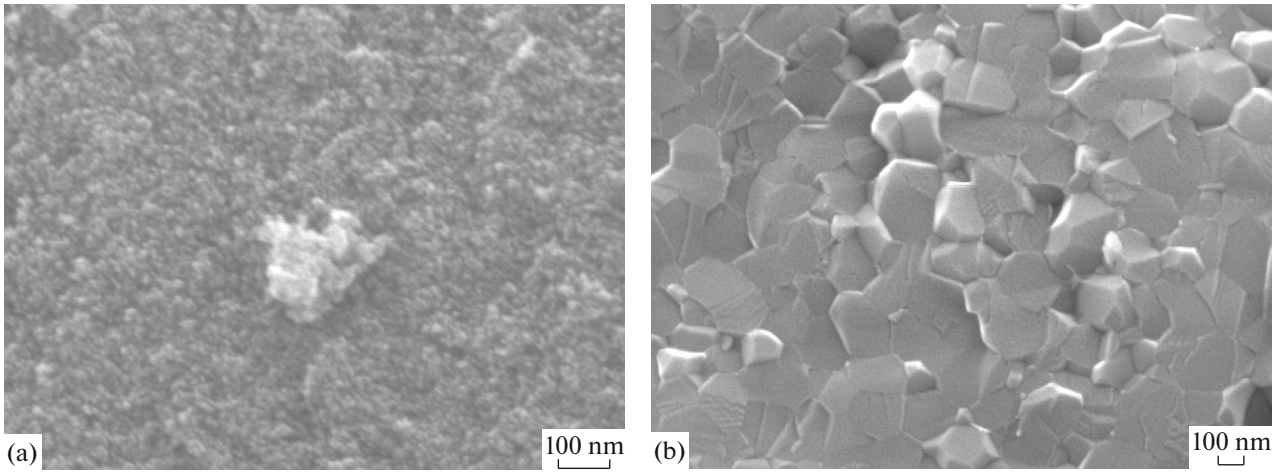

Fig. 2. Morphology sample IY02 after treatment at (a) 400°C (anatase) and (b) 1100°C (rutile) according to scanning electron microscopy data.

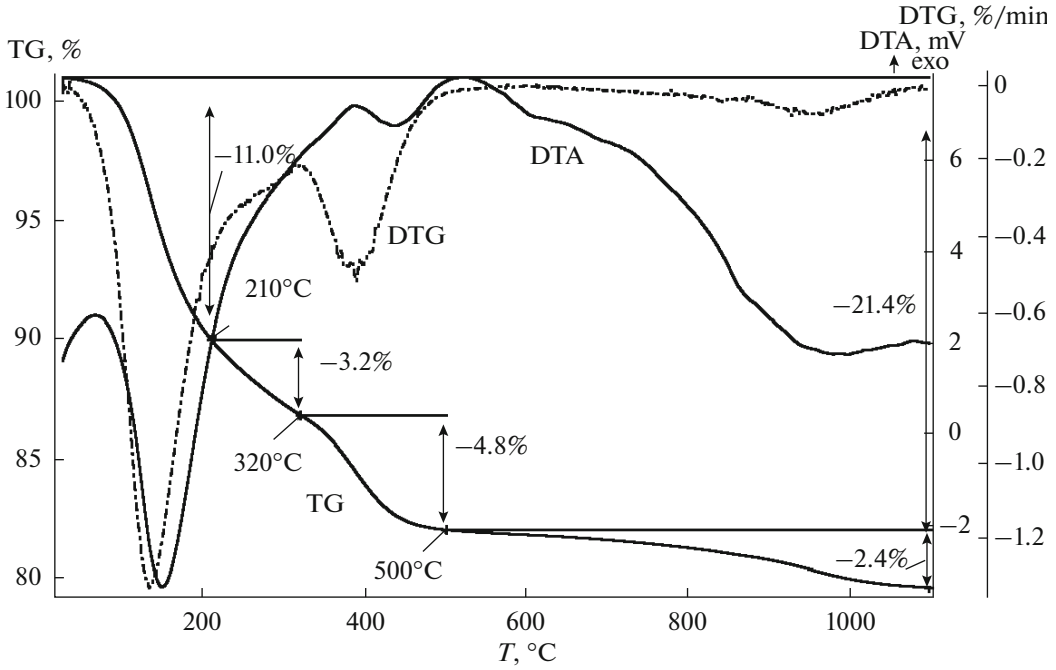

Fig. 3. Collective data of thermal studies of sample IY12 (250 mL of H_2O, 80°C): TG shows the change in the sample weight, DTG is the derivative of the TG signal, and DTA is the curve of the temperature difference between the sample and the empty crucible.

released; and at 210–320 and 320–500°C, the released products are water, butanol, ethanol, acac, and the products of the decomposition of organic compounds, including water and carbon dioxide. Within the range 500–1100°C, the weight slightly decreased without pronounced thermal events, which was due to the loss of traces of water and the oxidation of coked organic residues.

The double peak of the release of butanol may mean that the first, lower-temperature stage of the release of butanol with a maximum at 146°C is caused by the evaporation of the adsorbed butanol, which imparted a characteristic odor to the samples. The validity of this assumption is supported by the evaporation of similarly volatile water (not shown in Fig. 3) and ethanol within the same temperature range (the

butanol boiling point is 117°C) [10]. Likewise, acetylacetone, which has a higher boiling point (140°C) [10], has a peak of release at a somewhat higher temperature (192°C). The maximum of the second peak of the release of butanol is at 410°C and can be explained by the decomposition of nonhydrolyzed butoxyl groups bound to titanium. At higher temperatures, the oxidation to yield carbon dioxide with a maximum at about 420°C begins to dominate. The products of the thermolysis and coking of organic residues also manifest themselves as insignificant peaks corresponding to higher molecular weights (67–120 amu), which are not related to the above substances.

The second peak of the release of ethanol, similar to the second peak of the release of butanol, is most likely to characterize the decomposition of ethoxyl groups bound to titanium. This assumption agrees with the observation of the complex behavior of the hydrolysis, in particular, the temporary formation of a precipitate in pouring a TBT–acac–ethanol–water (samples IY11, 12, 15, 16, 19, and 20) to a large volume of water. Depending on the amounts of acac and water and also temperature, the precipitate exists for several seconds, after which it completely dissolves. Thus, we can state the partial substitution of ethoxyl and hydroxyl groups for butoxyl groups in the interaction with a water–alcohol solution, during which unstable insoluble intermediate compounds form.

The hydrolysis mechanism also depends on the formation of stable tri- and tetramers of TBT in solution [11, 12]. In this process, titanium atoms complete their coordination sphere to give an octahedron by forming donor–acceptor (bridging) bonds with oxygen atoms of neighboring TBT molecules. acac molecules with titanium alkoxides form strong complexes of the type $Ti(OBu)_3(acac)$ and $[Ti_2(\mu\text{-}OEt)_2(OBu)_4(acac)_2]$, which require much more water for hydrolysis of alkoxy groups than pure alkoxides [12]. The further stages of $Ti(OBu)_3(acac)$ hydrolysis with increasing water concentration include the formation of polynuclear titanium complexes with hydroxyl bridging groups and then with oxygen bridging groups, presumably of the type $[Ti_2(\mu\text{-}OH)_2(OBu)_4(acac)_2] \rightarrow [Ti_2(\mu\text{-}OH)_2(OBu)_2(OH)_2(acac)_2] \rightarrow [Ti_2(\mu\text{-}OH)_2(OH)_4(acac)_2]$. In the presence of acac, some of the alkoxy groups in these complexes are replaced by more strongly bound chelate molecules acac, which are the last to be hydrolyzed. Cluster $Ti_4O_2(OPr^i)_{10}(acac)_2$ was produced by slow hydrolysis of a 1 : 0.5 $Ti(OPr^i)_4$–acac mixture [12]. A larger-sized cluster $Ti_{18}O_{22}(OBu)_{26}(acac)_2$ was obtained by slow hydrolysis of a 1 : 0.1 $Ti(OBu)_4$–acac mixture. acac ligands protect polynuclear titanium clusters from further coarsening and growth by blocking peripheral positions to shield from from condensation.

In the reaction with water at the first stage, hydroxy groups are substituted for alkoxy groups. The validity of this assumption is supported by the fact that the hydrolysis at $Ti(OPr^i)_4$: acac = 1 : 2 gives compound $[Ti_2(\mu\text{-}O)_2(acac)_4]$ [12], for which the melting point and solubility in water were measured to be 200°C and 6.6 g/L at 20°C, respectively. This compound is a hydrolysis product in the hypothetical chain $[Ti(OR)_2(acac)_2] \rightarrow [Ti(OH)_2(acac)_2] \rightarrow [Ti_2(\mu\text{-}O)_2(acac)_4]$. It follows from this assumption that, in the slow hydrolysis of TBT in the presence of acac, butoxy groups should be the first to be hydrolyzed and removed, and acetylacetone should remain in solution much longer. Thus, increasing Ti : acac ratio from 1 : 0.1 to 1 : 2 in hydrolysis leads to a decrease in the degree of cluster condensation from $Ti_{18}O_{22}(OBu)_{26}(acac)_2$ to $Ti_2(\mu\text{-}O)_2(acac)_4$. The size of the latter cluster is about 1.5 nm.

In the experiments performed in this work, the volume ratios of 1 mL of TBT to 0.05, 0.1, 0.2, and 0.4 mL of acac correspond to the molar ratios TBT : acac = 0.167, 0.334, 0.668, and 1.337, respectively (the TBT and acac densities are 0.996 and 0.979 g/cm^3, respectively). Similarly, the volume ratios of 1 mL of TBT to 0, 0.5, 1, 2, and 4 mL water (taking into account water in 5 mL of 96 vol % alcohol) correspond to the molar ratios TBT : water = 4.64, 14.10, 23.57, 42.50, and 80.36, respectively.

Comparing the thermal curves of samples IY12, 19, and 20 with each other, one can conclude that heating of solutions to 80°C favors more complete hydrolysis and reduction of weight loss at all the stages. Increasing acac content also reduces weight loss at all the stages. The latter can be explained by the fact that, first, the rearrangement of amorphous particles from loose saturated hydroxyl, butoxy, and ethoxy groups into denser particles and their approach to more thermodynamically stable state and structure (anatase) occurs more rapidly when the rearrangement is facilitated by the formation of soluble complexes. Second, the bond of titanium with acac molecules is stronger than that with hydroxy and alkoxy groups, which may lead to their displacement from amorphous particles. For example, in sample IY20 in comparison with the other samples, there is much lower weight loss within the range 500–1100°C, in which hydroxyl groups are lost.

On the other hand, at relatively low temperatures, comparison of the gel weights after treatments at 50, 100, and 400°C showed that the weight of organic fragments and water after treatments at 50 and 100°C in the precipitate with respect to the TiO_2 weight (taken as 100%) with increasing acac concentration from 0.05 to 0.4 mL linearly increases from 10–15 to 20–30 wt % after treatment at 50°C and from 5–8 to 10–16 wt % after treatment at 100°C. Probably, with increasing acac content in the solution, the acac content of the amorphous particles also increases.

After heat treatment at 400°C, all the samples acquired an anatase structure (Fig. 4). From the broadening of the peaks, the sizes of coherent scatter-

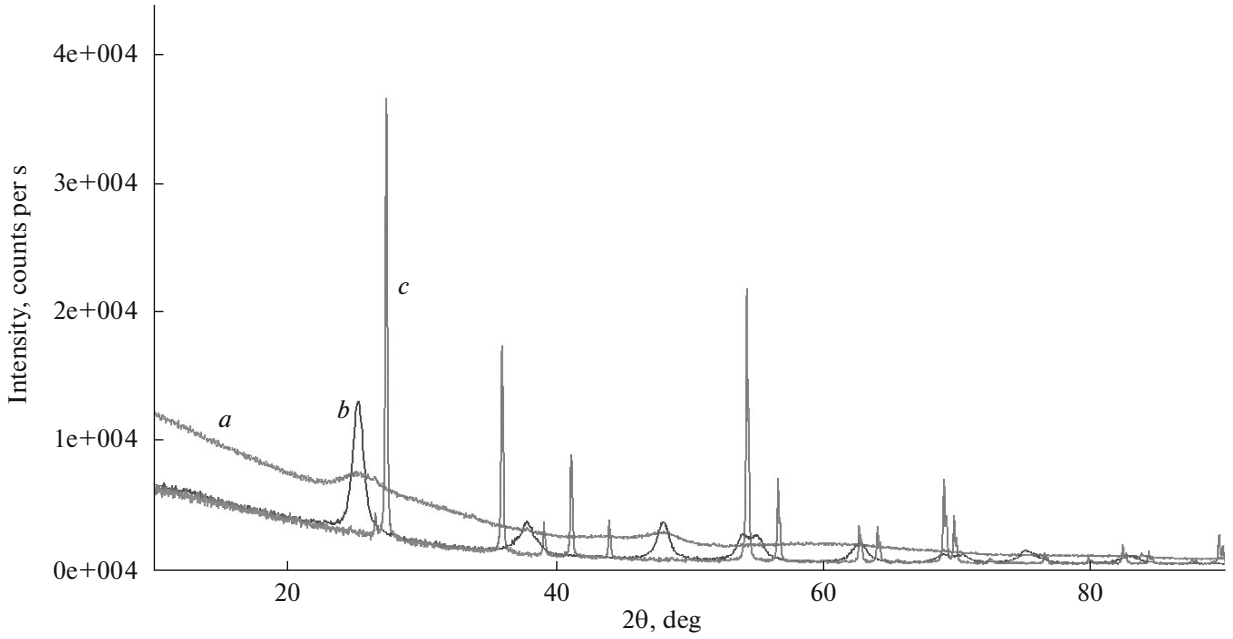

Fig. 4. X-ray powder diffraction patterns of sample IY04 after treatment at (*a*) 100 and (*b*) 400°C and (*c*) sample IY20 after treatment at 1100°C.

ing domains (TiO_2 crystallites) can be estimated at 6.2–8.4 nm. This size is almost independent of the acac content in the synthesis in the solution but somewhat increases with increasing water content.

For samples IY10–IY20, the absence of the stage of keeping for 7 days at 22°C before heating to 70°C also led to the formation of somewhat larger anatase crystallites. This may indicate either that, at lower temperature, more particle formation nuclei form in the solution, or that there is transfer of the material from the smaller to the larger particles. After heating to 1100°C, anatase transforms to more thermodynamically stable rutile with crystals about 250 nm in size (Fig. 2b). In the recrystallization from anatase to rutile, the crystal size increases by a factor of 30–40, the material is consolidated, and the porosity virtually vanishes.

The results of determining the adsorption properties of the obtained materials showed that, whatever the sample production conditions, the adsorption by all the annealed samples is approximately equal and is 9–15 g per 100 g of TiO_2. In estimating the porosity of the samples the geometric sizes (cylinder diameter and height) of which can be measured, it turned out that the pore volume per 1 g of TiO_2 corresponds with sufficient accuracy to the volume of the benzene adsorbed in the adsorption measurements. Thus, it can be concluded that, at a benzene vapor pressure of $P/P_0 = 0.69$, there is capillary filling of all the pores, the sizes of which in the synthesized materials can be estimated at 1–5 nm. Because in the close packing of equal spheres, the ratio between the pore volume and the sphere volume is independent of the sphere diameter, the benzene adsorption is virtually independent of the synthesis conditions.

In the isotherms of the nitrogen adsorption by samples IY07 and 08 (Fig. 5), hysteresis loops are clearly seen in the adsorption and desorption branches. For sample IY07, this stage in the adsorption isotherm corresponds to a narrow pore size distribution with a maximum at about 4.4 nm; and for sample IY08, 4.0 nm. These sizes correlate well with the crystal sizes by the data of X-ray powder diffraction analysis and electron microscopy. The specific surface areas of samples IY07 and IY08 according to the BET equation are 148.5 and 98 m^2/g, respectively.

Thus, in this work, we studied tetrabutoxy titanium hydrolysis in a water–ethanol mixture to give titanium oxyhydrate sol and gel. Introduction of acetylacetone to the hydrolysis medium enables one to reduce the tetrabutoxy titanium hydrolysis rate and obtain the product as spherical particles 5–9 nm in diameter. The nanoparticle size at the hydrolysis stage decreases with increasing acac concentration. After treatment at 400°C, amorphous samples crystallize in the anatase structure. According to X-ray powder diffraction data, the average crystallite size is 6.2–8.4 nm. It was shown that, after heating to 1100°C, anatase transforms to more thermodynamically stable rutile with crystals about 250 nm in size. Electron microscopy measurements and adsorption studies showed that the produced nanosized TiO_2 can be assigned to mesoporous nanomaterials with a pore size of about 250 nm. The specific surface area was found to be 148.5 and 98 m^2/g

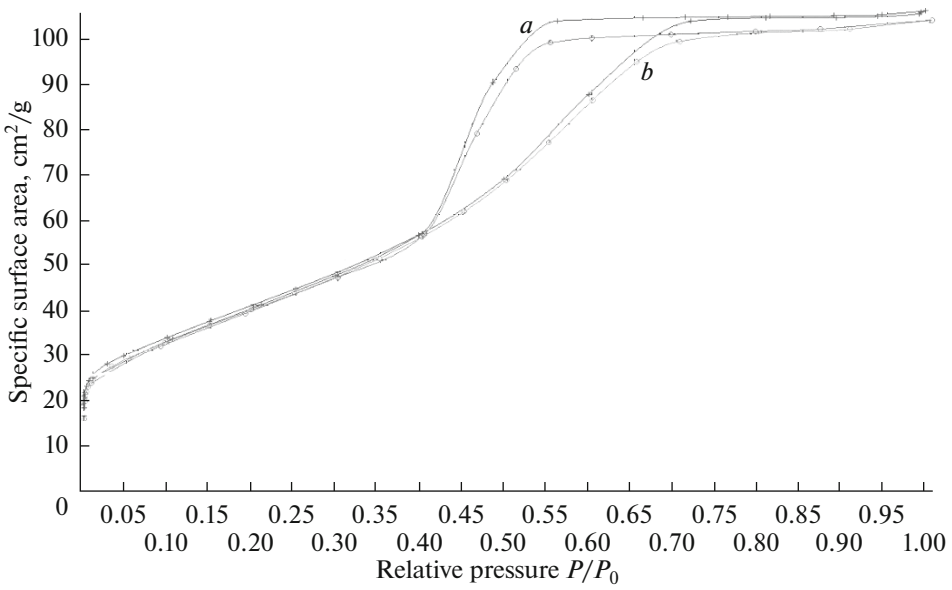

Fig. 5. Adsorption isotherms of samples (*a*) IY07 and (*b*) IY08.

for samples IY07 and IY08, respectively. It was confirmed that it is convenient to carry out the TBT hydrolysis in two stages, performing the preliminary hydrolysis to yield transparent gels in the presence of relatively high acetylacetone concentrations.

REFERENCES

1. J. S. Beck, J. C. Vartuli, W. J. Roth, et al., J. Am. Chem. Soc. **114**, 10834 (1992).
2. A. Fujishima, K. Hashimoto, and T. Watanabe, *TiO_2 Photocatalysis: Fundamentals and Applications* (BKC Inc., Tokyo, 1999).
3. J. M. Coronado, F. Fresno, M. D. Hernandez-Alonso, et al., *Design of Advanced Photocatalytic Materials for Energy and Environmental Applications* (Springer, London, 2013).
4. G. J. Soler-Illia, C. Sanchez, B. Lebeau, et al., Chem. Rev. **102**, 4093 (2002).
5. S. Yuan, Q. Sheng, J. Zhang, et al., Microp. Mesop. Mater. B, 93 (2005).
6. G. Hasegawa, K. Kanamori, K. Nakanishi, et al., J. Am. Ceram. Soc. **93**, 3110 (2010).
7. A. L. Linsebigler, G. Lu, and J. T. Yates, Chem. Rev. **95**, 735 (1995).
8. D. M. Antonelli and Y. J. Ying, Angew. Chem. Int. Ed. Eng. **34**, 2014 (1995).
9. D. A. Zherebtsov, S. B. Sapozhnikov, D. M. Galimov, et al., Russ. J. Phys. Chem. **89**, 840 (2015).
10. *Chemical Encyclopedia*, Ed. by I. L. Knunyants and N. S. Zefirov (Sov. entsiklopediya, Moscow, 1988–1998) [in Russian].
11. D. C. Bradley, R. Mehrotra, I. Rothwell, et al., *Alkoxo and Aryloxo Derivatives of Metals* (Academic, San Diego, 2001).
12. U. Schubert, Mater. Chem. **15**, 3701 (2005).

Translated by V. Glyanchenko